REPORT DOCUMENTATION PAGE			Form Approved OMB No. 0704-0188
Public reporting burden for this collection of information is estimated to average 1 hour per response, including the time for reviewing instructions, searching existing data sources, gathering and maintaining the data needed, and completing and reviewing the collection of information. Send comments regarding this burden estimate only, other aspect of this collection of information, including suggestions for reducing this burden, to Washington Headquarters Services, Directorate for Information Operations and Reports, 1215 Jefferson Davis Highway, Suite 1204, Arlington, VA 22202-4302, and to the Office of Management and Budget, Paperwork Reduction Project (07804-0188), Washington, DC 20503.			
1. AGENCY USE ONLY *(LEAVE BLANK)*	2. REPORT DATE 20 August 1999		3. REPORT TYPE AND DATES COVERED Professional Paper
4. TITLE AND SUBTITLE Modeling of Pulsed Thermography in Anisotropic Media			5. FUNDING NUMBERS
6. AUTHOR(S) Ignacio Perez Paul Kulowitch Steven Shepard			
7. PERFORMING ORGANIZATION NAME(S) AND ADDRESS(ES) Naval Air Warfare Center Aircraft Division 22347 Cedar Point Road, Unit #6 Patuxent River, Maryland 20670-1161			8. PERFORMING ORGANIZATION REPORT NUMBER
9. SPONSORING/MONITORING AGENCY NAME(S) AND ADDRESS(ES) Naval Air Systems Command 47123 Buse Road, Unit IPT Patuxent River, Maryland 20670-1547			10. SPONSORING/MONITORING AGENCY REPORT NUMBER
11. SUPPLEMENTARY NOTES			
12a. DISTRIBUTION/AVAILABILITY STATEMENT Approved for public release; distribution is unlimited.			12b. DISTRIBUTION CODE

13. ABSTRACT *(Maximum 200 words)*

Thermography is increasingly being used as an quantitative NDE tool to detect damage in materials. Most of the theoretical analysis performed on thermographic data involves the use of one dimensional models or finite element analysis. This is due to the inability to account for lateral heat effects in an analytical fashion. Three simple models have been developed that to a first order approximation describes the main features of thermal pulse analysis when applied to a planar flaws. The last and most general of the models introduced takes into account lateral heat conduction effects, anisotropic thermal conductivity, thickness effects, flaw size effects, density effects, material properties and pulse duration. The model correctly predicts the relationships between the previous parameters. Equations 4, 5, and 6 are the main output of the second model. These relations were shown to model correctly the time dependence of the thermal contrast, the peak thermal contrast, and the time at which the thermal contrast peaks.

14. SUBJECT TERMS			15. NUMBER OF PAGES
Thermography Anisotropic media			9
			16. PRICE CODE
17. SECURITY CLASSIFICATION OF REPORT	18. SECURITY CLASSIFICATION OF THIS PAGE	19. SECURITY CLASSIFICATION OF ABSTRACT	20. LIMITATION OF ABSTRACT
Unclassified	Unclassified	Unclassified	UL

MODELING OF PULSED THERMOGRAPHY IN ANISOTROPIC MEDIA

I. Perez, P. Kulowitch
Naval Air Warfare Center, Aircraft Division
Materials Division, Patuxent River MD, 20670

S. Shepard
Thermal Wave Imaging, Inc.
18899 W. 12 Mile Rd.
Lathrup Village, MI 48076

INTRODUCTION

Thermography is increasingly being used as an quantitative NDE tool to detect damage in materials. Most of the theoretical analysis performed on thermographic data involves the use of one dimensional models or finite element analysis. This is due to the inability to account for lateral heat effects in an analytical fashion.

In a previous paper [1] a simple model was developed (referred to as Model I) to describe the surface temperature evolution of a 1/8" thick aluminum panel with fixed 1" diameter flat bottom holes of different depth to a short pulse of radiant energy. That model correctly described the temporal behavior of all 1" flat bottom holes. To further validate Model I, a new panel was fabricated (Fig 1) that contained flat bottom holes of different diameters and different depths. After careful analysis of the data, it was found that Model I could not adequately account for the new experimental results. In this paper a new model will be introduced (referred to as Model II) and it will be shown that it accurately describes all experimental data. The main difference between both models is the way in which the thermal conductance's are modeled. In Model I the thermal conductance was approximated by an effective contact conductance ($K=k_c \cdot A$ where k_c is a contact conductivity and A is the cross sectional area). In Model II the thermal conductance is approximated by an effective thermal conductivity ($K=k \cdot A/l$ where k is the thermal conductivity and l is a characteristic length).

EXPERIMENTAL METHODS

The camera system used in this experiments was a liquid Nitrogen cooled Amber Engineering 4128 camera with silicon optics operating in the 3 - 5 micron region of the electromagnetic spectrum. The samples were thermally excited with a pair of Xenon Arc lamps, each one connected to a 5 KJoule capacitor bank with a 10 msec discharge time.

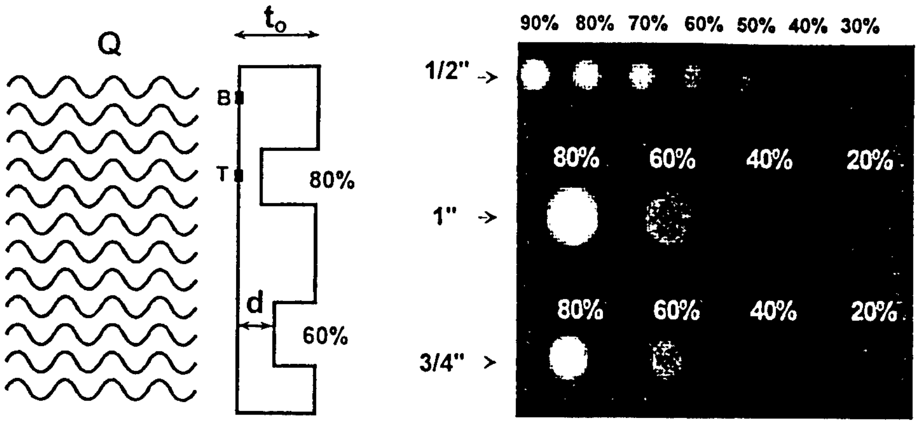

Figure. 1: The figure on the left shows a 1/8" thick aluminum Al -7075 panel with flat bottom holes of 1", ¾" and ½" diameters and various depth. The figure on the right shows a quasi-isotropic 1/8" thick graphite/epoxy composite with four flat bottom holes of ¼" diameter and various depths.

The material used in this study was a 1/8" thick aluminum panel with various 1", ¾" and ½" diameter flat bottom holes drilled at depths ranging from 25 mil to 100 mil in steps of 25 mil as shown in Fig 1. The center to center distance between flat bottom holes was set to at least 2 diameters to minimize hole proximity effects. The arc lamps were positioned so as to produce a uniform distribution of heat over the region being studied. The distance from the arc lamps to the sample was approximately 14". The distance from the camera to the samples was approximately 22". The data acquisition rate was 43 frames/sec and a total of 100 frames were collected for each experiment. Fig. 1 (Left) shows a drawing with the key parameters used in the study and model. The parameter "Q" represents the amount of energy deposited on the surface of the sample per unit area. The parameters "t_o" and "d" represent the thickness of the panel and the distance from the surface of the panel to the defect (the words "defect" and "flat bottom hole" will not be differentiated in this paper) respectively. The points "T" (just above a defect site) and "B" (far from any defect) are the points over the surface of the sample that where used to calculate the contrast curves (the contrast curve will be explained later). The quantity 80% and 60% represent the amount of material removed as a result of the drilling process. Fig. 1 (Right) shows an actual frame taken soon after the thermal flash was shot. The white areas in that photo represent the flat bottom holes that tend to remain hotter than the background material due to the fact that they are thinner.

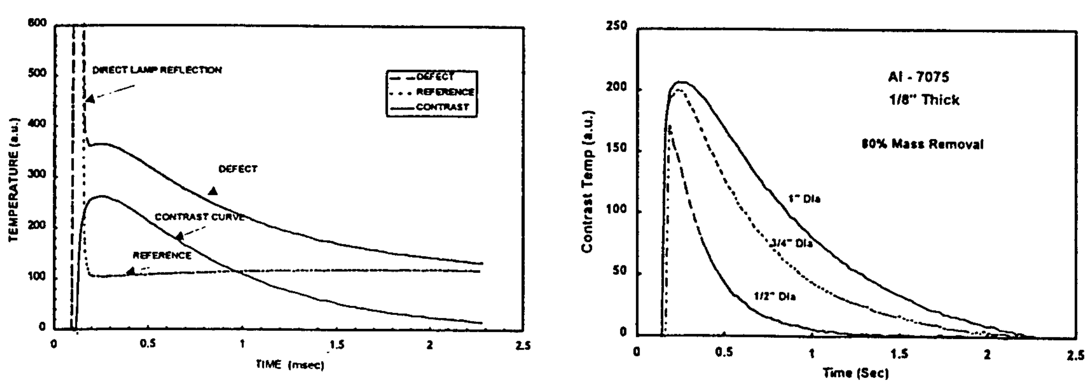

Figure. 2: (Left) This fig. shows the data curves require to generate a single contrast curve. (Right) This figure shows contrast curves for various flat bottom holes.

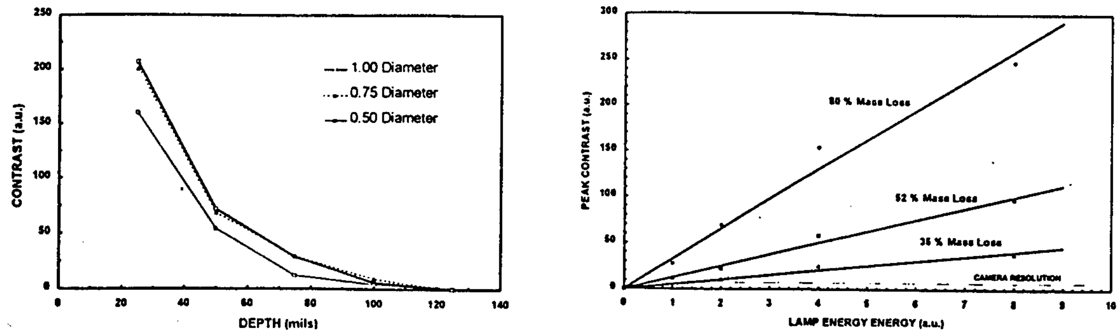

Figure. 3: (Left) This fig. show the evolution of the peak contrast as a function of the amount of material removed. (Right) This fig. shows the relation between the "peak contrast" and the amount of heat deposited in the surface of the material for three different defects.

EXPERIMENTAL RESULTS

In a standard experiment, the frame grabbing acquisition board is triggered first. After a few frames have been grabbed, the capacitor banks are discharged through the Xenon arc lamps. The grabbing rate is adjusted so that the entire thermal history (from room temperature to final equilibrium temperature) is recorded. In our experiments the frame rate was 43 frames/sec and the entire experiment lasted less than 2.5 sec. Fig. 2 Left shows the entire thermal history of two points on the surface of the panel. The curve labeled "defect" was taken from a point directly above and in the center of the flat bottom hole with 80% of material removed and it was referred as "T" in Fig. 1. This curve characterizes a typical damage site thermal evolution. The curve labeled "reference" was taken from a point far away from any flat bottom hole and characterizes the thermal history of an undamaged site, this point is referred as "B" in Fig. 1 (Left). Notice that the thermal history of the "reference" point does not decay monotonically as does the "defect" curve (there is a small increase in temperature in the reference curve at later times due to proximity effects). Also notice that the "reference" curve and the "defect" curve have a region at early times with very elevated temperature. This is an artifact produce by direct reflection of the initial flash produced by the arc lamps from the walls in the room to the camera and it normally disappears when calculating the contrast curve.

The difference of the "reference" curve from the "defect" curve is termed the "thermal contrast" curve and is the curve with a solid black line in Fig. 2 (Left). Thermal contrast curves start and end with zero temperature since the initial and final equilibrium temperatures are uniform throughout the entire panel. Fig. 2 (Right) shows contrast curves for three flat bottom holes with 1", ¾" and ½" diameters and 25 mil from the surface. It is clear from this figure that even though the distance from the surface of the panel to the defect is the same for those three flat bottom holes, the peak contrast temperatures and the overall shape of the curves are significantly different. It will be shown later on this paper that this differences can be modeled if the lateral heat effects are taken into account. Fig. 3 left shows the peak contrast temperatures for all flat bottom holes in the panel. The data points for the 1" and ¾" hole diameter almost overlap for all defect depth. The data for the ½" hole diameter is smaller than for the other holes.

Finally a set of experiments were performed where the amount of energy deposited on the surface of the sample was increased to study the relationship between peak thermal

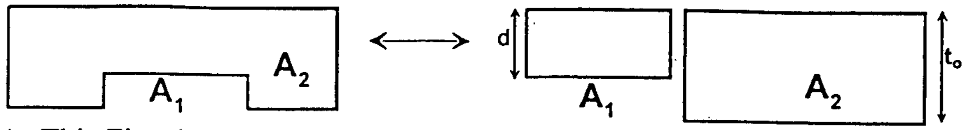

Figure. 4: This Fig. shows a schematic representation of the zero lateral flow assumption used in the model.

contrast and amount of delivered energy. Fig. 3 (Right) shows the results of this experiment for the 1" flat bottom holes. The amount of energy deposited on the surface of the panel was controlled by changing the amount of charge store in the capacitor banks. Four different settings were used which produced energy levels in the following amounts Q=1, Q=2, Q=4 and Q=8, where Q represents the amount of energy deposited per unit area (the energy is expressed in arbitrary units). From Fig. 3 (Right) it is clear that, for any given defect, as the energy deposited on the surface increases, the peak temperature contrast increases as well and in a linear proportion.

CALORIMETRIC MODEL (ZEROTH ORDER APPROXIMATION)

A simple theoretical model (zeroth order approximation) was introduced in our previous work [1] that, despite the fact that it was based in equilibrium thermodynamics and that no lateral heat effects were assumed, it correctly accounted for most of the observed experimental behavior of pulsed thermography. Fig. 4 shows a schematic representation of the model. Two regions are defined in the model (drilled and un-drilled regions) and it is assumed that no lateral energy flows between them. In the next section a more refined model will be derived that takes into account lateral heat transfer effects.

By using simple calorimetric arguments it can be written that $q_1 = m_1 c T_1$ and $q_2 = m_2 c T_2$ where q_1, m_1, and T_1 are the energy deposited on block 1, the mass of block 1 and the final temperature of block 1 (similar definitions hold for block 2). The initial temperature of the panel can be assumed to be zero degrees. The mass can be written in terms of the density as $m_1 = \rho A_1 d$ and $m_2 = \rho A_2 t_o$. If it is assumed that the energy deposited on the surface of the panel per unit area is constant, i.e., $q_1/A_1 = q_2/A_2 = Q$, then the final equilibrium temperature difference (or thermal contrast) between both blocks $T_1 - T_2 = \Delta T$ will be

$$\Delta T = \frac{Q}{\rho c}\left(\frac{1}{d} - \frac{1}{t_o}\right) \tag{1}$$

This equation correctly accounts for most of the observed experimental behavior of pulsed thermography, i.e.,

1. The contrast temperature (ΔT) increases linearly with the amount of energy deposited per unit area (Q).
2. The higher the specific heat-density of a material ($\rho c \uparrow$) the smaller the contrast temperature becomes ($\Delta T \downarrow$)
3. The closer the defect is to the surface ($d \rightarrow 0$) the larger that the contrast temperature becomes ($\Delta T \rightarrow \infty$).
4. As the defect depth approaches the panel thickness ($d \rightarrow t_o$) the contrast temperature vanishes ($\Delta T \rightarrow 0$).

5. For a given defect depth d, the thicker the panel ($t_o \to \infty$) the larger the contrast temperature ($\Delta T \to Q/\rho c d$).

CALORIMETRIC MODEL (FIRST ORDER APPROXIMATION)

In this section the previous model will be modified to allow for lateral heat flow effects. In this model it will be assumed that the in-plane thermal conductivity and the out-of-plane thermal conductivity are different. This will produce the most general results. In this model a poor man finite element (three elements only) approximation will be used but all the elements will be thermally interconnected. Fig. 5 shows a schematic representation of the heat flow model.

In this model it will be assumed that all the energy of the heat pulse is absorbed in a layer of thickness "d". This layer corresponds to the material above the defect and is represented by the hatched region in Fig. 5. As a result of this heating process, the initial temperature of this layer "T_o" can be derived from simple calorimetric argument from $Q = \rho \cdot c \cdot d \cdot T_o$ where it is assumed that the temperature of the panel before the heat pulse was zero degrees. The total thickness of the panel is given by $t_o = d + h$ where h represent the amount of material under the defect. In this model it is assumed that the in-plane material properties are isotropic but different from the out-of-plane properties. The quantities K and K_L are the normal and lateral thermal conductance's respectively. These quantities can be expressed in terms of the in-plane and out-of-plane thermal conductivities of the panel as

$$
\begin{aligned}
K &= k \cdot A_1/(d+h) \\
K_L &= k_L \cdot A_d/R
\end{aligned}
\qquad (2)
$$

where "k" is the normal (out-of-plane) thermal conductivity of the material being studied (in this case aluminum) while "k_l" is the lateral (in-plane) thermal conductivity (in the case of Aluminum $k = k_L$). These definitions of the thermal conductances are the main differences between this model and the one introduced previously [1]. A_1 and A_2 are shown in the figure and represent the surface area of the defect and the surface area of rest of the material respectively. A_1 can be written as $A_1 = \pi R^2$ where R is the radius of the flat bottom hole while A_2 will be assumed to tend to infinity ($A_2 \to \infty$). A_d is not shown explicitly in the figure but represent the lateral cross sectional areas and can be expressed as $A_d = 2\pi R \cdot d$. The set of differential equations that define this problem are

$$
\begin{aligned}
\rho \cdot A_1 \cdot d \cdot c \cdot \frac{dT_1}{dt} &= k_L \cdot \frac{A_L}{R}(T_2 - T_1) \\
\rho \cdot A_2 \cdot d \cdot c \cdot \frac{dT_2}{dt} &= k_L \cdot \frac{A_L}{R}(T_1 - T_2) + k \cdot \frac{A_2}{d+h}(T_2' - T_2) \\
\rho \cdot A_2 \cdot h \cdot c \cdot \frac{dT_2'}{dt} &= k \cdot \frac{A_2}{d+h}(T_2 - T_2')
\end{aligned}
\qquad (3)
$$

Where T_1, T_2 and T_2' are the temperatures of the different blocks as shown in Fig. 5. The

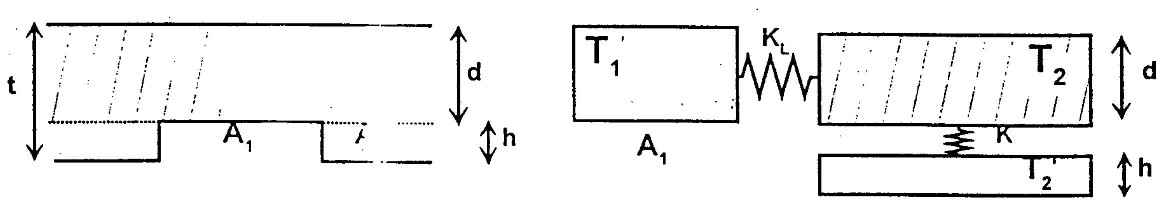

Figure. 5: This figure shows the building blocks of our simple model.

Where T_1, T_2 and T_2' are the temperatures of the different blocks as shown in Fig. 5. The boundary conditions of the problem are $T_1(t=0) = T_o$, $T_2(t=0) = T_o$, $T_2'(t=0) = 0$. This set of coupled differential equations can be easily solved in the limit when $A_2 \to \infty$ an the contrast curve $\Delta T(t) = T_1(t) - T_2(t)$ obtained from it is

$$\Delta T(t) = \frac{Q}{\rho c \cdot d \cdot (1 - a + r)} \left(e^{-\frac{a}{d(d+h)} \frac{k}{\rho c} t} - e^{-\frac{1+r}{d(d+h)} \frac{k}{\rho c} t} \right) \tag{4}$$

where $a = \frac{k_L}{k} \frac{A_d}{A_l} \frac{d+h}{R}$ and $r = \frac{d}{h}$ (don't confuse the variable "t = time" with the parameter "t_o = panel thickness").

The maximum or peak thermal contrast can be calculated by differentiating Eq. 4 and the result gives

$$\Delta T_{max} = \frac{Q}{\rho c} \left(\frac{1}{d} - \frac{1}{t_o} \right) \cdot \left[\frac{a \cdot h}{t_o} \right]^{\frac{1}{\frac{t_o}{a \cdot h} - 1}} \tag{5}$$

which happens at a time give by

$$t_{max} = \frac{\rho c}{k} \frac{d \cdot t_o}{1 - a + r} \ln \frac{1+r}{a}. \tag{6}$$

It is worth comparing eqs. 1 and 5. It can be seen from those equations that the lateral heat flow effects can be grouped as a multiplicative factor to the main contrast relation Eq. 1.

ANALYSIS OF RESULTS FOR ALUMINUM PANEL

To understand the effects that the lateral flow of heat has on the peak thermal contrast ΔT_{max}, eq. 5 needs to be studied further. If it is assumed that the material is isotropic then the lateral and normal thermal conductivity's will be the same. The parameter "a" can the be written as $a = A_d (d+h)/(A_l R) = 2d(t_o - d)/R^2$. The lateral heat flow contribution to the peak thermal contrast (the square bracket term in eq. 5) can then be simplified to

$$f_{lateral}(d) = \left[\frac{a \cdot h}{t_o} \right]^{\frac{1}{\frac{t_o}{a \cdot h} - 1}} = \left[\frac{2d \cdot (t_o - d)}{R^2} \right]^{\frac{1}{\frac{R^2}{2d(t_o - d)} - 1}}. \tag{7}$$

Fig. 6 shows a graph of Eq. 7 for various hole diameters as a function of defect

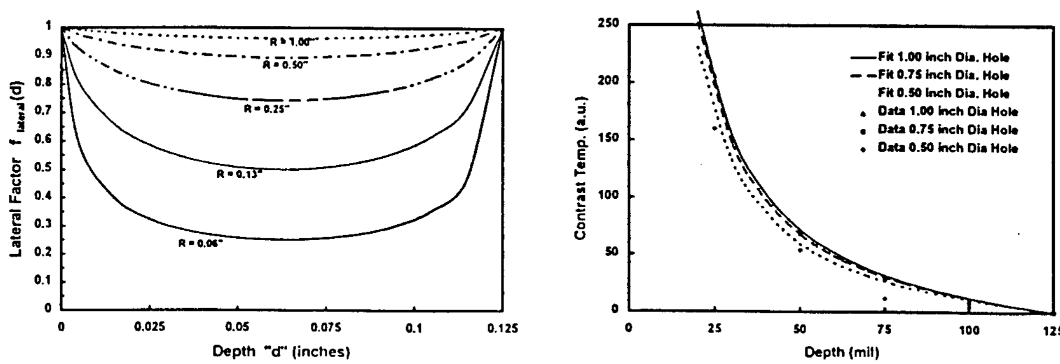

Fig. 6: This figure shows the lateral heat flow factor (Eq. 7) as a function of the depth of the flaw for various hole radii.

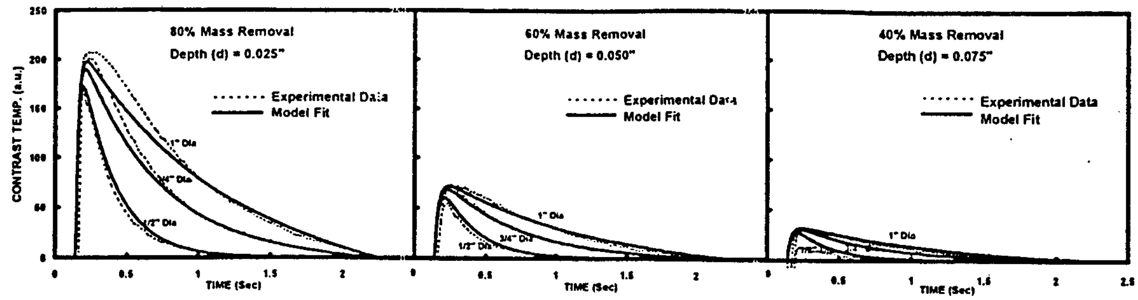

Figure. 7: This figure shows the fit (solid lines) to the experimental contrast curve data (doted lines). Each graphs shows the contrast curves for three flat bottom holes at constant depth but with different diameter holes.

depth. From there it can be seen that for flaws that are very close to the surface ($d \approx 0$) or for flaws that are very deep in the material ($d \approx t_o$) the lateral heat flaw effects tend to disappear in this model (or the lateral heat flow factor $f_{lateral}(d) \rightarrow 1$) and as a result all the contribution to the peak thermal contrast will come from Eq. 1 (which assumed no lateral heat flow). This result can be explained as follows: In the limit when $d \rightarrow 0$, the lateral conduction of heat will tend to zero because the lateral cross sectional area ($2\pi R \cdot d$) will become vanishingly small and therefore Eq. 1 is recovered. In the limit when $d \rightarrow t_o$, the lateral conduction of heat will tend to zero because in this limit the temperature gradients will approach zero and therefore Eq. 1 is recovered. Finally, when $R \rightarrow \infty$ the lateral conduction of heat will again tend to zero because of the length over which the thermal energy has to travel is large and therefore Eq. 1 is recovered.

Eq. 5 was used to fit the experimental values of the peak contrast introduced at the beginning of the paper. Fig. 6 shows the result of the fits (lines) to the three sets of data point. Only one parameter ($Q/\rho c$) was adjusted to fit all three data sets.

Eq. 4 was used to fit all the experimental contrast curves. From Fig. 7 it can be seen that this simple model fits fairly well the experimental thermal contrast curves. The only parameter that was adjusted to fit all contrast curves was the thermal conductivity normalized to the specific heat-density "$k/\rho c$". The best fit is for the data with 60% mass removal. The model does not fit the time period around the maximum for the 80% mass removal case.

QUASIISOTROPIC MATERIALS

To validate the model further, a 1/8" thick graphite epoxy composite panel was fabricated with four 0.5" diameter flat bottom holes at various depths. A standard heat pulse experiment was performed on the sample. After careful analysis of the data it was

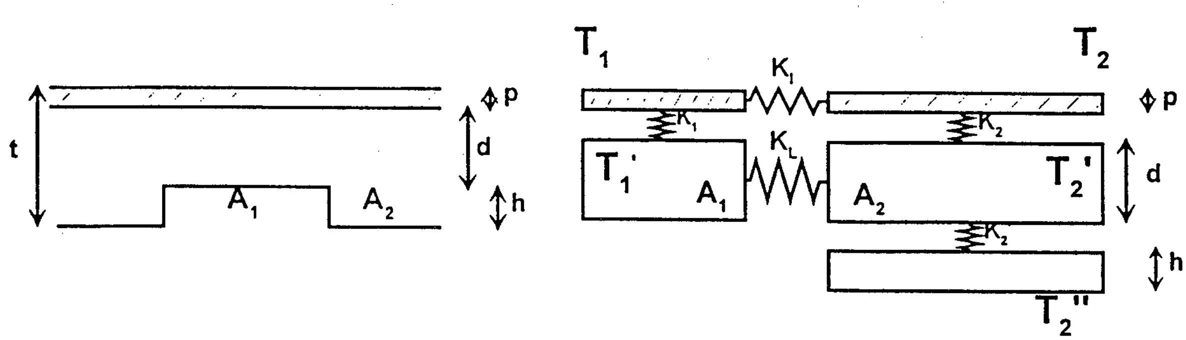

Figure 8: This figure shows the building blocks of our most general model.

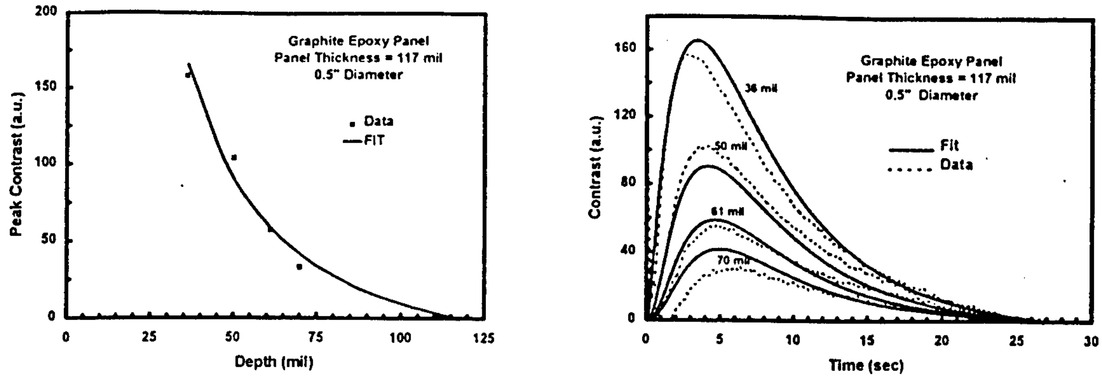

Figure 9: This figure shows the results of the fit of the new model to the four flat bottom holes in a graphite epoxy composite

found that our simple model (Eqs. 4, 5 and 6) was not able to adequately fit the data. Two factors are believed to be responsible to the discrepancies, the significantly larger thermal relaxation time of the Gr/Ep panel compared to the Aluminum panel and the larger in-plane thermal conductivity compared to the out-of-plane one. A new, more general model was developed. In this model (Fig. 8) it is assumed that the thickness of material over which the heat pulse is absorbed is a new variable defined by "p". A new set of differential equations can be written for this problem in the same fashion that were derived for the previous model (Eqs. 3). The thermal conductance's are defined in the same fashion as before (Eqs. 2). A closed form solution can be found for the temporal dependence of the thermal contrast (not shown here because of its length). A closed form solution for the peak thermal contrast and for the time at which the peak thermal contrast happens has not been found.

Figure 9 shows the results of this, more general model. The agreement between the data and the model is very good. Some of the small discrepancies found can be attributed to the difficulties of finding systematic background curves. Further studies need to be performed to validate the model.

CONCLUSION

Three simple models have been developed that to a first order approximation describes the main features of thermal pulse analysis when applied to a planar flaws. The last and most general of the models introduced takes into account lateral heat conduction effects, anisotropic thermal conductivity, thickness effects, flaw size effects, density effects, material properties and pulse duration. The model correctly predicts the relationships between the previous parameters. Eqs. 4, 5 and 6 are the main output of the second model. This relations were shown to model correctly the time dependence of the thermal contrast, the peak thermal contrast and the time at which the thermal contrast peaks.

ACKNOWLEDGEMENTS

This work was supported by Mr. Jim Kelly from the Office of Naval Research by Work Request under document number N0001498WX20360.

REFERENCES

[1] "Calorimetric Modeling of Thermographic Data," I. Perez, R. Santos, P. Kulowitch, M. Ryan, Proceeding of the Thermosense conference